

## AN EFFICIENT MOVING MESH METHOD FOR A MODEL OF TURBULENT FLOW IN CIRCULAR TUBES\*

Yin Yang

*Hunan Key Laboratory for Computation and Simulation in Science and Engineering, School of  
Mathematics and Computational Science, Xiangtan University, Xiangtan 411105, China*

*Email: yangyin.xtu@xtu.edu.cn*

Yanping Chen

*School of Mathematical Sciences, South China Normal University, Guangzhou, China*

*Email: yanpingchen@scnu.edu.cn*

Yunqing Huang

*Hunan Key Laboratory for Computation and Simulation in Science and Engineering, School of  
Mathematics and Computational Science, Xiangtan University, Xiangtan 411105, China*

*Email: huangyq@xtu.edu.cn*

### Abstract

This paper presents an efficient moving mesh method to solve a nonlinear singular problem with an optimal control constrained condition. The physical problem is governed by a new model of turbulent flow in circular tubes proposed by Luo *et al.* using Prandtl's mixing-length theory. Our algorithm is formed by an outer iterative algorithm for handling the optimal control condition and an inner adaptive mesh redistribution algorithm for solving the singular governing equations. We discretize the nonlinear problem by using a upwinding approach, and the resulting nonlinear equations are solved by using the Newton-Raphson method. The mesh is generated and the grid points are moved by using the arc-length equidistribution principle. The numerical results demonstrate that proposed algorithm is effective in capturing the boundary layers associated with the turbulent model.

*Mathematics subject classification:* 65L10, 65L12.

*Key words:* Eddy viscosity, Turbulent pipe flow, Boundary layer, Optimal control, Moving mesh.

### 1. Introduction

The modeling of turbulent flows still plays an important role in computational fluid dynamics because direct simulation of flows are restricted to very simple geometries and low Reynolds number [6, 9, 18, 19]. Development of turbulence model is therefore still an important task and even some semi-empirical means such as the eddy viscosity or Prandtl's mixing length are very helpful to deal with many problems in engineering practice due to their simplicity. Luo *et al.* [15] established a new model of turbulent flow in circular tubes which is an application and improvement of Prandtl's mixing-length theory. The model expresses the single phase flow in circular tubes, which is an optimal parameter control problem governed by a nonlinear singular equation. The model yields many complex mathematical characters such as strong boundary layer. The computational results resulting from the new model are found in good agreement with the experimental results on fluid velocity distribution, eddy viscosity distribution and friction factor. On the mathematical side, the governing equations associate with this model

---

\* Received January 5, 2008 / Revised version received August 5, 2008 / Accepted September 5, 2008 /

are quite complicated, and an effective numerical scheme for finding numerical approximations seems useful.

The difficulties of this problem include the existence of the boundary layers and an optional control condition enforced on the governing equations. To resolve the layers, numerical simulations require extremely fine meshes on the small localized portions of the physical domain. It will become very expensive if a uniform fine mesh is employed. Recent study has demonstrated that moving mesh methods are powerful in resolving large solution variations by increasing the solution accuracy and decreasing the cost of computations, see, e.g., Adaptive moving mesh methods have important applications in solving partial differential equations (PDEs). Up to now, there have been important progresses [1, 3, 20]. Harten and Hyman [11] began the earliest study of the adaptive methods to improve resolution of discontinuous solutions of hyperbolic equations. After their work, many other moving mesh methods on this direction have been proposed based on combining the variational grid methods with high resolution shock capturing methods, including the so-called moving mesh PDE (MMPDE) approach of moving mesh methods of W. Huang [10], moving finite element methods of Miller [17], and moving finite volume methods [22]. Recently, there have been works on moving mesh methods based on Harmonic maps [8, 16, 22]. Theoretical results on adaptive mesh arising from equidistribution of a monitor function can be found in [3, 4, 12–14, 21]. In particular, Kopteva [13] derived certain maximum norm a posteriori error estimates for one-dimensional singularly perturbed convection-diffusion problems, see also a recent paper [14] for a similar posterior error estimate.

The aim of this paper is to present an efficient and fast numerical method for the turbulent model. The proposed numerical algorithm includes two parts: (i) the outer iterative algorithm is used to solve the optimal control condition and (ii) the inner adaptive mesh redistribution algorithm is used to solve the singular problem. We discretize this nonlinear problem by using upwinding scheme. The discretized nonlinear equations is solved by Newton-Raphson method. The arc-length equidistribution principle is used in the part (ii) above. The numerical examples will be provided to demonstrate the effectiveness of the proposed algorithm.

This paper is organized as follows. In Section 2, we briefly review the model of turbulent flow in circular tubes by employing Prandtl's mixing-length theory. In Section 3, we will present the discrete schemes and algorithms. Numerical experiments will be carried out in Section 4. Some concluding remarks will be presented in the final section.

## 2. A New Model of Turbulent Flow in Circular Tubes

In this section, we briefly review the background of the model of turbulent flow in circular tubes which was proposed by Luo *et al.* [15]. Moreover, using dimensionless analysis we will derive a complete mathematical description for this model.

Note that the shearing stress of Newtonian fluid for turbulent flow can be described by eddy viscosity with dimensionless analysis [9]. We then have following expression:

$$\frac{d\tilde{u}}{d\phi} = \frac{-\hat{R}\phi}{1 + \mu_t/\mu_L}, \quad (2.1)$$

where  $\tilde{u}$  is dimensionless time-smoothed velocity,  $\mu_t$  is eddy viscosity,  $\mu_L$  is kinematic viscosity,  $\hat{R}$  is dimensionless radius of a circular pipe and  $\hat{R} = \rho\hat{u}R/\mu$  with  $R$  is the tube radius,  $\rho$  is the liquid density,  $\hat{u}$  is friction velocity,  $\mu$  is the molecule viscosity,  $\phi$  is dimensionless radial position in a circular pipe,  $\phi = 0$  is the center of the tube and  $\phi = 1$  corresponds to the wall of

the tube. As the velocity is disappeared on the wall, we have the boundary condition

$$\tilde{u}(\phi)|_{\phi=1} = 0. \quad (2.2)$$

Based on Prandtl's mixing-length theory, the eddy viscosity can be written as

$$\frac{\mu_t}{\mu_L} = \hat{R} \frac{L}{R} \left| \frac{L}{R} \frac{d\tilde{u}}{d\phi} \right|, \quad (2.3)$$

and the constrained condition is

$$2 \int_0^1 \tilde{u}\phi d\phi = \frac{\bar{u}}{\hat{u}} = \frac{Re}{\hat{R}}, \quad (2.4)$$

where  $L$  is the mixing length,  $\bar{u}$  is average velocity in cross section of tubes,  $Re$  is the Reynolds number defined by  $Re = \rho\bar{u}R/\mu$ . Let  $\lambda = L/R$  be the dimensionless mixing length. Then (2.3) can be rewritten as

$$\frac{\mu_t}{\mu_L} = \hat{R}\lambda \left| \lambda \frac{d\tilde{u}}{d\phi} \right|. \quad (2.5)$$

Coupling (2.1) and (2.5), we have the following equation which is the application of the classical Prandtl's mixing-length,

$$\frac{d\tilde{u}}{d\phi} = \frac{-\hat{R}\phi}{1 + \hat{R}\lambda \left| \lambda \frac{d\tilde{u}}{d\phi} \right|}. \quad (2.6)$$

Set  $\tilde{u}'(\phi) = d\tilde{u}/d\phi$ . Then (2.6) can be written as

$$\tilde{u}'(\phi) = \frac{-\hat{R}\phi}{1 + \hat{R}\lambda \left| \lambda \tilde{u}'(\phi) \right|}. \quad (2.7)$$

Using the symmetry of turbulent flow, we have

$$\left. \frac{d\tilde{u}}{d\phi} \right|_{\phi=0} = 0.$$

It can be seen from Eq. (2.5) that the eddy viscosity  $\mu_t$  at the center of a circular tube will be zero. However, the eddy viscosity at the center is non-zero according to either the conception or the experiment. This inconsistency may be caused mainly by the fact that the Prandtl theory only took the first-order derivative of velocity to approximate the eddy velocity (2.5). Thus, Luo *et al.* [15] introduced a simple way to modify the Prandtl's mixing length theory by utilizing the second-order derivative to approximate the eddy velocity. By doing this, Eq. (2.5) can be changed to

$$\frac{\mu_t}{\mu_L} = \hat{R}\lambda \left| \lambda \tilde{u}'(\phi) + \frac{1}{2} \lambda^2 \tilde{u}''(\phi) \right|. \quad (2.8)$$

Combining (2.1) and (2.8) yields

$$\tilde{u}'(\phi) = \frac{-\hat{R}\phi}{1 + \hat{R}\lambda \left| \lambda \tilde{u}'(\phi) + \frac{1}{2} \lambda^2 \tilde{u}''(\phi) \right|}. \quad (2.9)$$

The dimensionless mixing length  $\lambda$  in (2.9) is found to be not a universal constant but a function of position,

$$\lambda = L/R = kf(\phi), \quad f(\phi) \geq 0, \quad f(0) = 1, \quad f(1) = 0, \quad (2.10)$$

where  $k$  is a dimensionless positive constant.

For single phase flow in circular tubes, so  $\tilde{u}'$  and  $\tilde{u}''$  are nonpositive, the absolute sign in (2.9) can be dropped. Then (2.9) can be rewritten as

$$\tilde{u}'(\phi) \left[ 1 - \hat{R}(kf(\phi))^2\tilde{u}'(\phi) - \hat{R}(kf(\phi))^3\tilde{u}''(\phi) \right] = -\hat{R}\phi. \tag{2.11}$$

Since

$$\left( 1 - \hat{R}(kf(\phi))^2\tilde{u}'(\phi) - \hat{R}(kf(\phi))^3\tilde{u}''(\phi) \right) \Big|_{\phi=0} > 0,$$

and

$$\tilde{u}'(0) \left( 1 - \hat{R}(kf(0))^2\tilde{u}'(0) - \hat{R}(kf(0))^3\tilde{u}''(0) \right) = 0,$$

we can derive that (2.11) satisfies the symmetry of the turbulent flow:

$$\tilde{u}'(0) = 0. \tag{2.12}$$

We then obtain from (2.11) that

$$1 - \hat{R}k^2 f(\phi)^2 \tilde{u}'(\phi) - \hat{R}k^3 f(\phi)^3 \tilde{u}''(\phi) = -\frac{\hat{R}\phi}{\tilde{u}'(\phi)}, \quad \phi \in (0, 1]. \tag{2.13}$$

Set  $a(\phi) = \hat{R}k^2 f(\phi)^2$  and  $b(\phi) = \hat{R}k^3 f(\phi)^3$ . Letting  $\phi \rightarrow 0$  in (2.13) gives

$$\begin{aligned} \lim_{\phi \rightarrow 0} (1 - a(\phi)\tilde{u}'(\phi) - b(\phi)\tilde{u}''(\phi)) &= \lim_{\phi \rightarrow 0} \frac{-\hat{R}\phi}{\tilde{u}'(\phi)} \\ &= (1 - b(0)\tilde{u}''(0)) = \frac{-\hat{R}}{\tilde{u}''(0)} \quad (\text{using L' Hospital rule}). \end{aligned}$$

Then we obtain that

$$\tilde{u}''(0) = \frac{1 - \sqrt{1 + 4b(0)\hat{R}}}{2b(0)} = \frac{1 - \sqrt{1 + 2\hat{R}^2 k^3}}{\hat{R}k^3}. \tag{2.14}$$

For the turbulent flow,  $Re \in (4000, 10000)$ . In (2.10),  $k$  and  $f(\phi)$  have many possible choices. Because we are aimed at showing how to solve the non-linear singular model (2.11) with an optimal control condition (2.4), we use the expression proposed by Prandtl. When the Reynolds number is sufficiently high, the mixing length in the wall turbulence can be written as

$$f(\phi) = 1 - \phi, \quad k = 0.2. \tag{2.15}$$

Then we change the problem to the following mathematical model. For any given  $\alpha \in (4000, 10000)$ , find constant  $c$  such that  $y$  satisfy

$$y'(x) \left( 1 - k^2 c(1 - x^2)^2 y'(x) - \frac{1}{2} k^3 c(1 - x^2)^3 y''(x) \right) = -cx, \quad x \in [0, 1] \tag{2.16}$$

and the constrained condition

$$2 \int_0^1 xy dx = \frac{\alpha}{c}, \tag{2.17}$$

together with three boundary conditions

$$y(1) = 0, \quad y'(0) = 0, \quad y''(0) = \frac{1 - \sqrt{1 + 2c^2 k^3}}{ck^3}. \tag{2.18}$$

It is easy to show that  $c > 0$ . Set  $x = 1$  in (2.16), it can be verified that

$$y'(1) = -c. \quad (2.19)$$

Since  $y'(x)$  and  $y''(x)$  are nonpositive,  $k$  and  $c$  are positive, we have

$$y'(x) \leq 0, \quad (2.20a)$$

$$\left(1 - k^2 c (1 - x^2)^2 y'(x) - \frac{1}{2} k^3 c (1 - x^2)^3 y''(x)\right) \geq 0, \quad (2.20b)$$

$$-cx \leq 0. \quad (2.20c)$$

It is then expected that we have the boundary condition  $y'(0) = 0$  and  $y'(x)$  has no other zero point. Moreover,  $x = 1$  is the singular point of the equation, which may yield a boundary layer on the right end.

### 3. A Moving Mesh Algorithm

In this section, we present an efficient and fast approach for the model (2.16)-(2.18), which includes an iterative method and an adaptive method.

#### 3.1. Analysis of the model

We consider the model (2.16)-(2.17). The difficulty of this problem involves two parts. Firstly,  $c$  is unknown as well as  $y$ ; this problem is an optimal control problem and (2.17) is a control equation. For a given  $\alpha$ , we want to obtain the solution  $y$  and  $c$  which not only satisfy the differential equation (2.16) but also the control (2.17). Secondly, (2.16) is not only a nonlinear differential equation, but also a singular problem.

In order to solve the optimal control problem, we use an iterative algorithm to compute  $y$  and  $c$ . For an initial  $c_0$ , solve (2.16) to obtain  $y$ . Then compute  $c$  by solving (2.17) with the obtained  $y$ . Compare the computed  $c$  and the initial  $c_0$ , if the discrepancy satisfies an preassigned tolerance, stop computing, else, the obtained  $c$  becomes the initial value and repeat the process. This is an outer iteration for solving the model. A detailed algorithm will be described in the next subsection.

Then we consider Eq. (2.16) with boundary conditions in (2.18). As a singular problem, there is a region in which the solution of the differential equation is steep. For  $(1 - x^2) \ll 1$  when  $x \rightarrow 1$ , the solution has a boundary layer near the boundary  $x = 1$ . It is well known that central or upwinding differential scheme on an uniform mesh will not give a satisfactory numerical solution in this case. To obtain a reliable numerical solution for (2.16) and (2.18), it is better to use a mesh that concentrates nodes in the boundary layer. Ideally, the mesh should be generated by adapting it to the features of the computed solution and this is usually done by equidistributing a monitor function over the domain of the problem. This adaptive methods can handle not only boundary layer but also interior layer problems. In fact, this is a moving mesh approach that can capture the layer effectively.

#### 3.2. Numerical method and algorithm

Given a partition of  $[0, 1]$ :

$$\Omega_N = \{x_j | 0 = x_0 < x_1 < \cdots < x_N = 1\}.$$

On  $\Omega_N$ , we discretize (2.16) and (2.18) by using a upwinding scheme as follows:

$$D^+y_i(1 - a_iD^+y_i - b_iDD^-y_i) = -cx_i \quad \text{for } 1 \leq i \leq N - 1 \tag{3.1}$$

with  $y_N = 0$ , where the operators used are given by

$$\begin{aligned} D^-v_i &= \frac{v_i - v_{i-1}}{h_i}, & D^+v_i &= \frac{v_{i+1} - v_i}{h_{i+1}}, & Dv_i &= \frac{v_{i+1} - v_i}{\bar{h}_i}, \\ h_i &= x_i - x_{i-1}, & \bar{h}_i &= (h_{i+1} + h_i)/2, \\ a_i &= k^2c(1 - x_i^2)^2, & b_i &= \frac{1}{2}k^3c(1 - x_i^2)^3. \end{aligned}$$

At  $x = 0$ , since

$$y'(x) \approx y'(0) + xy''(0) = xy''(0),$$

we set

$$y''(0) \approx \frac{\frac{y_0 - y_{-1}}{h_1} - \frac{y_1 - y_0}{h_1}}{h_1} = 2\frac{y_1 - y_0}{h_1^2},$$

where  $y_{-1} = y_1$  is used. Consequently, the discretization of (2.16) at  $x = 0$  becomes

$$2\frac{y_1 - y_0}{h_1^2} \left(1 - b_0 2\frac{y_1 - y_0}{h_1^2}\right) = -c. \tag{3.2}$$

As Eq. (3.1) is a nonlinear equation, we use Newton-Raphson iteration method to solve it. The integration in (2.17) is approximated by the following quadrature formula:

$$2 \int_0^1 xydx \approx \sum_0^N h_i(x_i y_i + x_{i-1} y_{i-1}). \tag{3.3}$$

Denote  $y_i(x) \in C[0, 1]$  the piecewise linear interpolant through the knots  $(x_i, y_i)$ . We choose a monitor function:

$$w(x) = \sqrt{1 + |y'_i(x)|^2}$$

to equidistribute mesh which is the discrete analogue of the standard arc-length monitor function

$$w(x) = \sqrt{1 + |y'(x)|^2}.$$

Note that

$$(y_i(x))' = D^-y_i, \quad x \in I_i = (x_{i-1}, x_i), \quad 1 \leq i \leq N - 1.$$

In an other words, we construct a mesh by solving the following equations:

$$\begin{aligned} (x_{i+1} - x_i)^2 + (y_{i+1} - y_i)^2 &= (x_i - x_{i-1})^2 + (y_i - y_{i-1})^2, \quad 1 \leq i \leq N - 1, \\ x_0 = 0, \quad x_N = 1. \end{aligned} \tag{3.4}$$

To equidistribute the mesh and to capture the boundary layer, we move mesh iteratively to generate a fine mesh.

**Main Algorithm**

1. Initialize  $c_0$  and give mesh  $\Omega_N$ ;
2. Use Newton-Raphson method and call adaptive algorithm to compute the discrete solution  $\{y_i\}$  by (3.1) on  $\Omega_N$ ;
3. Solve  $c = \frac{\alpha}{2 \int_0^1 xy dx}$  by (3.3) , if  $|c - c_0| \leq \eta$ , goto step 5, otherwise continue;
4. Set  $c_0 = \sqrt{c \times c_0}$ , return to step 2;
5. Set  $c = c_0$ , then stop.

**Adaptive Algorithm**

1. Initialize mesh:  $\Omega_N^{(0)} = \{x_j^{(0)} | 0 = x_0^{(0)} < x_1^{(0)} < \dots < x_N^{(0)} = 1\}$ ,  $k = 0$ ;
2. Solve (3.1) for  $\{y_i^{(k)}\}$ , let

$$l_i^{(k)} = \sqrt{(y^{(k)}(x_i^{(k)}) - y^{(k)}(x_{i-1}^{(k)}))^2 + (h_i^{(k)})^2}, \quad L^{(k)} = \sum_{i=1}^N l_i^{(k)}.$$

3. Test mesh: let  $\tau$  be a user chosen constant with  $\tau > 1$ . If  $\max l^{(k)}/L^{(k)} \leq \tau/N$ , then goto step 5.
4. Generate new mesh: choose point  $0 = x_0^{(k+1)} < x_1^{(k+1)} < \dots < x_N^{(k+1)} = 1$ , such that for each  $i$ , the distance from  $(x_{i-1}^{(k+1)}, y^{(k)}(x_{i-1}^{(k+1)}))$  to  $(x_i^{(k+1)}, y^{(k)}(x_i^{(k+1)}))$  equals  $L^{(k)}/N$ . Let  $k = k + 1$ , return to step 2.
5. Set  $x_i = x_i^{(k)}$ ,  $y_i = y_i^{(k)}$ , then stop.

**4. Numerical Results**

This section considers numerical solutions of the model (2.16)-(2.17) to demonstrate the performance of the iterative method and the moving mesh method proposed in last section. The parameters  $\alpha$  in (2.17) are taken as 2000, 4000, 6000, 8000, 10000 respectively. For a given  $\alpha$ , there is a corresponding  $c$  satisfying (2.16)-(2.17). Table 4.1 and Fig. 4.1 show the relation between  $\alpha$  and  $c$ . From Table 4.1, we conclude that  $c$  is monotonically increasing with respect to  $\alpha$  for a fixed  $N$  and  $c$  is convergent with increasing  $N$ . Fig. 4.1 shows that the relation of  $\alpha$  and  $c$  is almost linear. So using least-square methods we can write  $\alpha$  and  $c$  in the form of  $c = k\alpha + b$  with  $k = 0.079$  and  $\alpha = 110.24$ .

Table 4.1: The value of  $c$  for different  $\alpha$  and different  $N$ .

$N$	$\alpha = 2000$	$\alpha = 4000$	$\alpha = 6000$	$\alpha = 8000$	$\alpha = 10000$
64	249.36	434.97	606.60	769.94	927.64
128	245.98	428.30	596.61	756.84	910.98
256	244.31	425.02	591.73	750.13	902.87
512	243.38	423.51	589.26	746.92	898.89
1024	242.99	422.66	588.31	745.48	897.06
2048	242.99	422.66	588.31	745.46	897.03

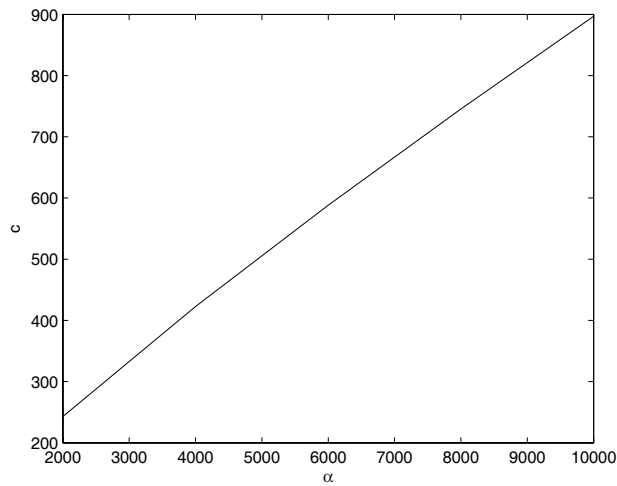


Fig. 4.1. The relation of dimensionless radius  $c$  and the Reynold number  $\alpha$ .

In this model  $y(x)$  is the velocity distribution. Eq. (2.16) is a nonlinear convection-dominated stationary convection-diffusion problem. The solution  $y(x)$  to (2.16) and (2.18) has a boundary layer near  $x = 1$ . Our numerical solution  $\{y_i\}$  showing by Fig. 4.2 confirms that  $\{y_i\}$  is very steep near  $x = 1$ .

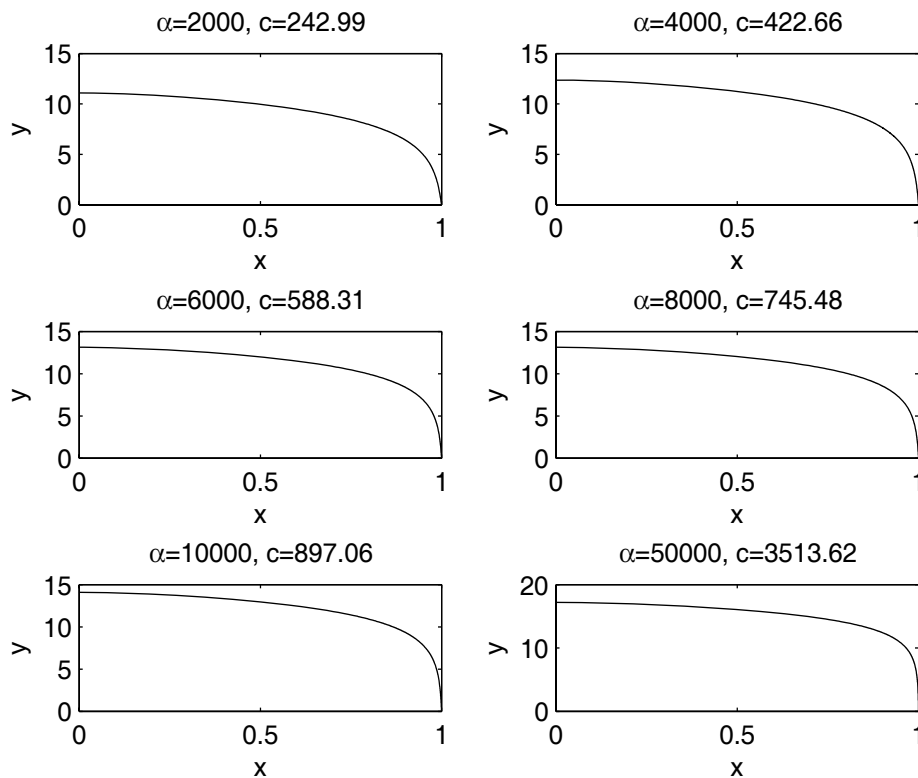


Fig. 4.2. Liquid velocity distribution  $y$  for different Reynold number  $\alpha$ .

With the boundary condition  $y'(0) = 0$  and since  $y'(x)$  may have no other zero point, we change Eq. (2.16) to

$$\left(1 - k^2c(1 - x^2)^2y' - \frac{1}{2}k^3c(1 - x^2)^3y''\right) = -\frac{cx}{y'}, \quad x \in (0, 1].$$

Set

$$z(x) = \left(1 - k^2c(1 - x^2)^2y' - \frac{1}{2}k^3c(1 - x^2)^3y''\right) = -\frac{cx}{y'}, \quad x \in (0, 1]. \quad (4.1)$$

At  $x = 0$ , by (2.18), we have

$$z(0) = \frac{-c}{y''(0)} = \frac{1 + \sqrt{1 + 2k^3c^2}}{2}.$$

Note that  $z(x)$  is the eddy viscosity distribution. Let  $z_i$  be the discrete form of  $z(x)$ . Then we have

$$\begin{aligned} z_0 &= \frac{1 + \sqrt{1 + 2k^3c^2}}{2}, \\ z_i &= -\frac{cx_i h_{i+1}}{y_{i+1} - y_i}, \quad \text{for } i = 1, \dots, N - 1, \\ z_N &= z(1) = \left. \frac{-cx}{y'(x)} \right|_{x=1} = \frac{-c}{-c} = 1. \end{aligned}$$

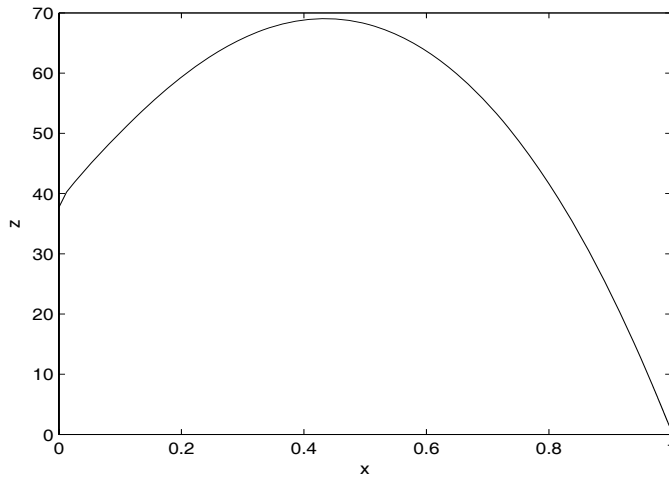


Fig. 4.3. The eddy viscosity distribution  $z$  for Reynold number  $\alpha = 6000$ .

Denote  $z_i(x)$  the piecewise linear interpolation though the knots  $(x_i, z_i)$ . Fig. 4.3 presents the value of  $z(x)$  in the case of  $\alpha = 6000$  with  $N = 1024$ . Fig. 4.4 shows the whole history of the mesh moving from its initial uniform mesh and the convergence history of  $c$  from its initial value  $c = 1.0$ . It is clearly demonstrated that the mesh concentrates nodes near the boundary layer.

From Fig. 4.4, it is observed that for  $c = 1.0$  the mesh move from the uniform mesh to the 1st level mesh; for  $c = 156$  the mesh moves from 2nd to 3rd mesh while the 3rd mesh is the final adaptive mesh corresponding to  $c = 156$ . The mesh of 6th level is good enough for other

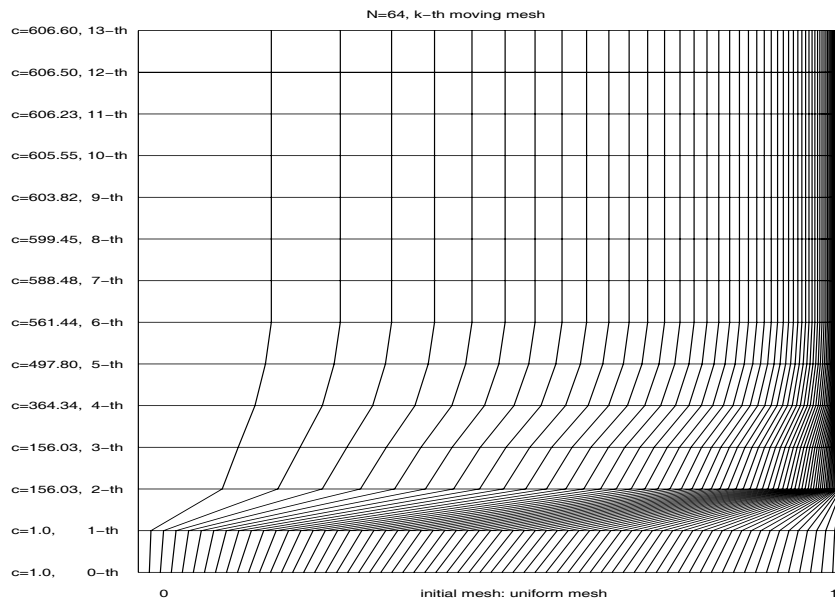


Fig. 4.4. Moving mesh history.

choices of  $c$ , so only outer iterations are needed to compute the convergent  $c$  while the mesh does not need to move any more.

In our algorithm, for a fixed  $\alpha$ ,  $c$  can be convergent from an arbitrary initial value. Taking  $\alpha = 6000$  for example, the following datum shows how  $c_0 = 1$  and  $c_0 = 1000$  convergence respectively with  $N = 1024$ :

$$\begin{aligned}
 c_0 = 1.0 &\rightarrow 156.35 \rightarrow 358.95 \rightarrow 487.13 \rightarrow 547.38 \rightarrow 572.81 \rightarrow 582.81 \rightarrow 586.51 \\
 &\rightarrow 587.88 \rightarrow 588.20 \rightarrow 588.24 \rightarrow 588.27 \rightarrow 588.29 \rightarrow 588.30 \rightarrow 588.31. \\
 c_0 = 10000 &\rightarrow 1904.78 \rightarrow 944.58 \rightarrow 710.318 \rightarrow 634.28 \rightarrow 596.04 \rightarrow 591.98 \\
 &\rightarrow 590.40 \rightarrow 589.79 \rightarrow 588.50 \rightarrow 588.37 \rightarrow 588.32 \rightarrow 588.31.
 \end{aligned}$$

Our outer iterative is mainly to compute  $c$  and  $y$ . Take  $\alpha = 6000$  and  $N = 1024$  with initial  $c_0 = 1.0$  as an example. Fig. 4.5 gives the convergent velocity of  $c$  by plotting  $\log(|c - c_0|)$ , where  $c$  is computed by the present iterative value,  $c_0$  the last iterative value. We can find that its convergence is almost linear.

We close this section by making several remarks. First, in the main algorithm, we have another choice of step 4, i.e., set  $c_0 = c$ , return to step 2. Secondly, in the Newton-Raphson iteration, we choose the initial guess for  $y_i^{(0)} = 0$  and  $y_i^{(0)} = 1$ ; both give the same convergent value. Thirdly, in step 3 of the adaptive algorithm,  $\tau$  can be chosen that to satisfy  $\tau \geq 1$ . In this paper, we set  $\tau = 1.1$ .

### 5. Conclusions and Future Works

In this paper, following a new proposal of Luo *et al.* [15] the mathematical governing equations for a model for turbulent flow in circular tubes are derived. The mathematical setting involves a nonlinear singular problem with an optimal control condition. An efficient numerical strategy based on the moving mesh method is proposed. The numerical results show that

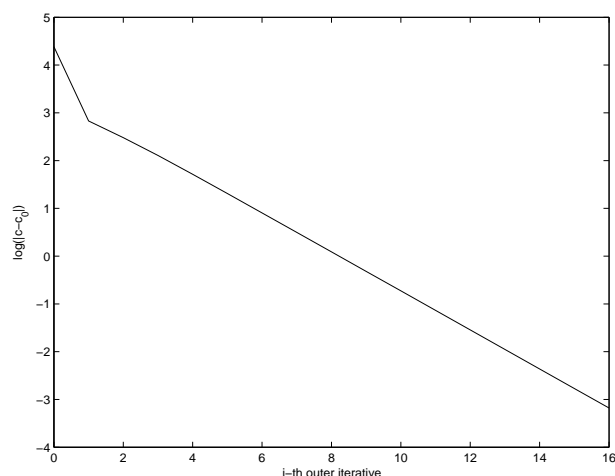


Fig. 4.5. Variation of  $\log(|c - c_0|)$  vs.  $i$ -th outer iteration.

our proposed numerical scheme is efficient in solving the nonlinear singular problem with constraints. In our future work, we will consider the theoretical aspects of the proposed method including issues on stability and accuracy.

**Acknowledgments.** We thank Professors Hean Luo, Pingle Liu and Xiao Luo for many helpful discussions during the preparation of this work. We would also like to thank the referees for very constructive comments. This work is supported by NSFC Outstanding Youth Scientist Grant 10625106 and NSFC grant 10671163, the National Basic Research Program of China under the grant 2005CB3217(01,03), and Scientific Research Fund of Hunan Provincial Education Department. Special thanks go to Guangdong Provincial "Zhujiang Scholar Award Project" awarded to the second author.

## References

- [1] J.U. Brackbill and J.S. Saltzman, Adaptive grid with directional control, *J. Comput. Phys.*, **108** (1993), 38-50.
- [2] M. Beckett and J.A. Mackenzie, Convergence analysis of finite difference approximations on equidistributed grids to a boundary value problem, *Appl. Numer. Math.*, **35** (2000), 87-109.
- [3] H.D. Ceniceros and T.Y. Hou, An efficient dynamically adaptive mesh for potentially singular solutions, *J. Comput. Phys.*, **172** (2001), 609-639.
- [4] Y. Chen, Uniform pointwise convergence for a singularly perturbed problem using arc-length equidistribution, *J. Comput. Appl. Math.*, **159** (2003), 25-34.
- [5] Y. Chen, Uniform convergence analysis of finite difference approximations for singular perturbations on an adaptive grid, *Adv. Comput. Math.*, **24** (2006), 197-212.
- [6] R. Datta, Eddy viscosity and velocity distribution in turbulent pipe flow revisited, *AICHE J.*, **39** (1993), 1107-1112.
- [7] S.F. Davis and J.E. Flaherty, An adaptive finite element method for initial boundary value problems for partial differential equations, *SIAM J. Sci. Comput.*, **3** (1982), 6-27.
- [8] Y. Di, R. Li and T. Tang, A general moving mesh framework in 3D and its application for simulating the mixture of multi-phase flows. *Commun. Comput. Phys.*, **3** (2008), 582-602.
- [9] U. Frisch, Turbulence, *Cambridge University Press*, (1995).

- [10] W.Z. Huang, Y. Ren and R. Russell, Moving mesh partial differential equations (MMPDEs) based on the equidistribution principle, *SIAM J. Numer. Anal.*, **31** (1994), 709-730.
- [11] A. Harten and J.M. Hyman, Self-adjusting grid methods for one-dimensional hyperbolic conservation laws, *J. Comput. Phys.*, **50** (1983), 235-269.
- [12] N. Kopteva, Maximum norm a posteriori error estimates for a one-dimensional convection-diffusion problem, *SIAM J. Numer. Anal.*, **39** (2001), pp. 423-441.
- [13] N. Kopteva and M. Stynes, A robust adaptive method for a quasi-linear one-dimensional convection-diffusion problem, *SIAM J. Numer. Anal.*, **39** (2001), 1446-1467.
- [14] T. Lin $\beta$ , Maximum-norm error analysis of a non-monotone FEM for a singularly perturbed reaction-diffusion problem, *BIT*, **47** (2007), 379-391.
- [15] X. Luo, P. Liu and H. Luo, Modeling of turbulent flow in circular tubes—the application and improvement of Prandtl's mixing-length theory, *J. Cent. South Univ. T. (English Edition)*, submitted.
- [16] R. Li, T. Tang and P.W. Zhang, Moving mesh methods in multiple dimensions based on Harmonic maps, *J. Comput. Phys.*, **170** (2001), 562-588.
- [17] K. Miller and R.N. Miller, Moving finite element I, *SIAM J. Numer. Anal.*, **18** (1981), 1019-1032.
- [18] Y.S.M. Morsi, P.G. Holland, B.R. Clayton, Prediction of turbulent swirling flows in axisymmetric annuli, *Appl. Math. Model.*, **19** (1996), 613-620.
- [19] T. Mizushima, F. Ogino, Eddy viscosity and universal velocity profile in turbulent flow in a straight pipe, *Journal of Chemical Engineering of Japan*, **35** (1970), 166-170.
- [20] Z.-H. Qiao, Numerical investigations of the dynamical behaviors and instabilities for the Gierer-Meinhardt system. *Commun. Comput. Phys.*, **3** (2008), 406-426.
- [21] Y. Qiu, D.M. Sloan and T. Tang, Numerical solution of a singularly perturbed two-point boundary value problem using equidistribution: analysis of convergence, *J. Comput. Appl. Math.*, **116** (2000), 121-143.
- [22] H.Z. Tang, T. Tang and P.W. Zhang, An adaptive mesh redistribution methods for non-linear Hamilton-Jacobi equations in two- and three-dimensions, *J. Comput. Phys.*, **188** (2003), 543-572.